REPORT DOCUMENTATION PAGE

Form Approved OMB NO. 0704-0188

1. REPORT DATE (DD-MM-YYYY)	2. REPORT TYPE	3. DATES COVERED (From - To)
18-03-2011	Final Report	23-Sep-2010 - 22-Mar-2011

4. TITLE AND SUBTITLE

Resonant Cavity Enhanced On-Chip Raman Spectrometer Array with Precisely Positioned Metallic Nano-Gaps for Single Molecule Detection

5a. CONTRACT NUMBER

5b. GRANT NUMBER

W911NF-10-C-0122

5c. PROGRAM ELEMENT NUMBER

665502

6. AUTHORS

Alan Wang, Donglei Fan, Ray T Chen

5d. PROJECT NUMBER

5e. TASK NUMBER

5f. WORK UNIT NUMBER

7. PERFORMING ORGANIZATION NAMES AND ADDRESSES

Omega Optics, Inc.
10435 Burnet Rd.
Suite 108
Austin, TX 78758 -4450

8. PERFORMING ORGANIZATION REPORT NUMBER

9. SPONSORING/MONITORING AGENCY NAME(S) AND ADDRESS(ES)

U.S. Army Research Office
P.O. Box 12211
Research Triangle Park, NC 27709-2211

10. SPONSOR/MONITOR'S ACRONYM(S)

ARO

11. SPONSOR/MONITOR'S REPORT NUMBER(S)

58703-EL-ST1.1

12. DISTRIBUTION AVAILIBILITY STATEMENT

Approved for Public Release; Distribution Unlimited

13. SUPPLEMENTARY NOTES

The views, opinions and/or findings contained in this report are those of the author(s) and should not contrued as an official Department of the Army position, policy or decision, unless so designated by other documentation.

14. ABSTRACT

During the Phase I program, our theoretical and experimental investigation has yielded fruitful results, which laid a solid foundation for the continuation of the Phase II program. From the design point of view, we designed ultra-compact highly reflective Si3N4 waveguide gratings with minimized side lobe reflection, and simulated the surface plasmonic resonance from metallic nanowires using 2-dimensional finite difference time domain (2-D FDTD) method. These simulation results have worked as the guideline for the Phase I experimental activities, and

15. SUBJECT TERMS

surface enhanced Raman scattering, nanowire, fiber-optic

16. SECURITY CLASSIFICATION OF:			17. LIMITATION OF ABSTRACT	15. NUMBER OF PAGES	19a. NAME OF RESPONSIBLE PERSON
a. REPORT	b. ABSTRACT	c. THIS PAGE			Alan Wang
UU	UU	UU	UU		19b. TELEPHONE NUMBER: 512-996-8833

Report Title

Resonant Cavity Enhanced On-Chip Raman Spectrometer Array with Precisely Positioned Metallic Nano-Gaps for Single Molecule Detection

ABSTRACT

During the Phase I program, our theoretical and experimental investigation has yielded fruitful results, which laid a solid foundation for the continuation of the Phase II program. From the design point of view, we designed ultra-compact highly reflective Si3N4 waveguide gratings with minimized side lobe reflection, and simulated the surface plasmonic resonance from metallic nanowires using 2-dimensional finite difference time domain (2-D FDTD) method. These simulation results have worked as the guideline for the Phase I experimental activities, and will continue to guide the Phase II program. In the aspects of device fabrication, we fabricated multi-segment gold nanowires with different diameters using electroplating, and formed nanogaps from 5nm to 50nm by sacrificial chemical etching. Surface enhanced Raman scattering (SERS) characterization using these gold nanowires with nanogaps are conducted to measure the Raman signals from Methylene Blue (MB) molecules.

List of papers submitted or published that acknowledge ARO support during this reporting period. List the papers, including journal references, in the following categories:

(a) Papers published in peer-reviewed journals (N/A for none)

Number of Papers published in peer-reviewed journals: 0.00

(b) Papers published in non-peer-reviewed journals or in conference proceedings (N/A for none)

Number of Papers published in non peer-reviewed journals: 0.00

(c) Presentations

Number of Presentations: 0.00

Non Peer-Reviewed Conference Proceeding publications (other than abstracts):

Number of Non Peer-Reviewed Conference Proceeding publications (other than abstracts): 0

Peer-Reviewed Conference Proceeding publications (other than abstracts):

Number of Peer-Reviewed Conference Proceeding publications (other than abstracts): 0

(d) Manuscripts

Number of Manuscripts: 0.00

Patents Submitted

Patents Awarded

Awards

Graduate Students

NAME	PERCENT_SUPPORTED
Xiaobin Xu	0.50
FTE Equivalent:	**0.50**
Total Number:	**1**

Names of Post Doctorates

NAME	PERCENT_SUPPORTED
FTE Equivalent:	
Total Number:	

Names of Faculty Supported

NAME	PERCENT_SUPPORTED	National Academy Member
Ray T. Chen	0.01	No
Donglei Fan	0.10	No
Alan Wang	0.25	No
FTE Equivalent:	**0.36**	
Total Number:	**3**	

Names of Under Graduate students supported

NAME	PERCENT_SUPPORTED
FTE Equivalent:	
Total Number:	

Student Metrics

This section only applies to graduating undergraduates supported by this agreement in this reporting period

The number of undergraduates funded by this agreement who graduated during this period:	0.00
The number of undergraduates funded by this agreement who graduated during this period with a degree in science, mathematics, engineering, or technology fields:.....	0.00
The number of undergraduates funded by your agreement who graduated during this period and will continue to pursue a graduate or Ph.D. degree in science, mathematics, engineering, or technology fields:.....	0.00
Number of graduating undergraduates who achieved a 3.5 GPA to 4.0 (4.0 max scale):	0.00
Number of graduating undergraduates funded by a DoD funded Center of Excellence grant for Education, Research and Engineering:	0.00
The number of undergraduates funded by your agreement who graduated during this period and intend to work for the Department of Defense	0.00
The number of undergraduates funded by your agreement who graduated during this period and will receive scholarships or fellowships for further studies in science, mathematics, engineering or technology fields:	0.00

Names of Personnel receiving masters degrees

NAME
Total Number:

Names of personnel receiving PHDs

NAME
Total Number:

Names of other research staff

NAME	PERCENT_SUPPORTED
FTE Equivalent:	
Total Number:	

Sub Contractors (DD882)

Inventions (DD882)

Scientific Progress

During the Phase I program, our theoretical and experimental investigation has yielded fruitful results, which laid a solid foundation for the continuation of the Phase II program. From the design point of view, we designed ultra-compact highly reflective Si3N4 waveguide gratings with minimized side lobe reflection, and simulated the surface plasmonic resonance from metallic nanowires using 2-dimensional finite difference time domain (2-D FDTD) method. These simulation results have worked as the guideline for the Phase I experimental activities, and will continue to guide the Phase II program. In the aspects of device fabrication, we fabricated multi-segment gold nanowires with different diameters using electroplating, and formed nanogaps from 5nm to 50nm by sacrificial chemical etching. Surface enhanced Raman scattering (SERS) characterization using these gold nanowires with nanogaps are conducted to measure the Raman signals from Methylene Blue (MB) molecules.

Technology Transfer

Resonant Cavity Enhanced On-Chip Raman Spectrometer Array with Precisely Positioned Metallic Nano-Gaps for Single Molecule Detection

Final Report

Reporting Period: September 23rd, 2010 – March 22nd, 2011

Contract No.: W911NF-10-C-0122

Technical Point of Contact

Dr. Alan X. Wang
Principal Investigator
alan.wang@omegaoptics.com

Dr. Donglei Fan
Co-Principal Investigator
dfan@austin.utexas.edu

Dr. Ray T. Chen
Consultant
raychen@uts.cc.utexas.edu

Tel: 512-996-8833 (602)

Fax: 512-873-7744

Contractual Point of Contact

Ray T. Chen

Phone: 512-825-4480

Fax: 512-873-7744

ray.chen@omegaoptics.com

Contract No: W911NF-10-C-0122
Contractor Name: Omega Optics, Inc.
Address: 10306 Sausalito Dr., Austin, TX 78759
Contract expiration date: Mar 22nd, 2011
Total dollar value: $99,999
Government sponsor: US ARMY RDECOM ACQ CTR

1. *Introduction*

The great potential of Surface Enhanced Raman Scattering (SERS) has not been materialized owing to the lack of plasmonic nanostructures that can not only provide extraordinary local field enhancements, but allow for a reproducible manufacturing with a high yield in large quantity. Studies have shown that large field enhancements are usually localized at the nanogaps of dimmer nanoantennas and increase dramatically when the gap size is below 5 nano-meter (nm). Early single molecule SERS experiments are done typically with aggregates of colloidal nanoparticles where the "hot-spots" of enhanced local fields are obtained only by chance, which is stoicastic and not controllable. From device engineering point of view, it is not a manufacturable technology. The particular challenge to achieving repeatable and controllable SERS active substrates originates from the difficulty to fabricate nanogaps controllably in large scale.

In this Phase I program, Omega Optics Inc. and the University of Texas at Austin propose a manufacturable resonant cavity enhanced (RCE) on-chip SERS array with precisely positioned metallic nano-gaps, which can achieve 10^{12} enhancement factor (EF) for single molecule detection. The proposed approach is anticipated to result in the realization of miniaturized on-chip integrated SERS solutions for lab-on-chip applications.

2. *Phase I Achievements*

During the Phase I program, our theoretical and experimental investigation has yielded fruitful results, which laid a solid foundation for the continuation of the Phase II program. From the design point of view, we designed ultra-compact highly reflective Si_3N_4 waveguide gratings with minimized side lobe reflection, and simulated the surface plasmonic resonance from metallic nanowires using 2-dimensional finite difference time domain (2-D FDTD) method. These simulation results have worked as the guideline for the Phase I experimental activities, and will continue to guide the Phase II program. In the aspects of device fabrication, we fabricated multi-segment gold nanowires with different diameters using electroplating, and formed nanogaps from 5nm to 50nm by sacrificial chemical etching. Surface enhanced Raman scattering (SERS) characterization using these gold nanowires with nanogaps are conducted to measure the Raman signals from Methylene Blue (MB) molecules.

2.1 Design of high reflectivity waveguide grating

Optical resonance has been used for biological sensing and imaging. The objective of this task is to design a resonant cavity on Si3N4 waveguide with enhanced optical intensity inside the cavity. The distributed Bragg reflective (DBR) mirrors are formed by etching quarter wave gratings on the polymer waveguide. According to Bragg's law, the intensity reflectivity of the DBR mirror is given by:

$$R = \tanh^2(N \cdot \frac{\Delta n}{n}) \qquad (1)$$

where N is the number of grating period, Δn is the effective refractive index between the high index and low index regions of the grating, and n is the average effective refractive index of the grating.

In our Phase I program, we used commercial software (Rsoft GratingMod) to simulate the performance of waveguide gratings, which can give a better precision and design flexibility. There are two basic types of optical gratings, as shown in Figure 2.1 (a) and (b).

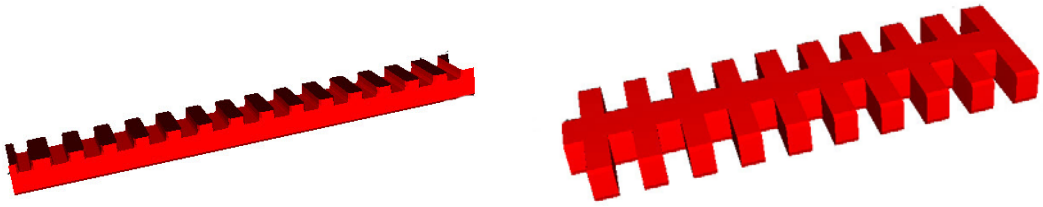

(a) (b)

Figure 2.1 Two types of optical waveguide gratings (a) top etched (b) laterally etched

The designed optical waveguide gratings will use materials with refractive indices given as:

Waveguide core materials: Si_3N_4, n=2.05
Bottom cladding materials: SiO_2, n=1.45
Top cladding materials: air, n=1

In Figure 2.1 (a), the waveguide dimension is 1μm×0.6μm, and the etching depth is 0.3μm. In Figure 2.1 (b), the waveguide dimension is 1μm×0.6μm as well, and the grating width is 3μm. Both waveguide gratings have a period of 0.2μm. Figure 2.2 (a) and (b) shows the calculated reflectivity of the waveguide gratings with 50 periods, or 10μm in length. Both gratings achieve excellent reflectivity of 99.99% and 99.78% within a very short length of 10μm. However, from the engineering point of view, laterally etched grating requires only one step of lithography and etching, and thus it is much easier for fabrication. In our design and experiments, we will focus on laterally etched gratings and optimize its reflection spectrum.

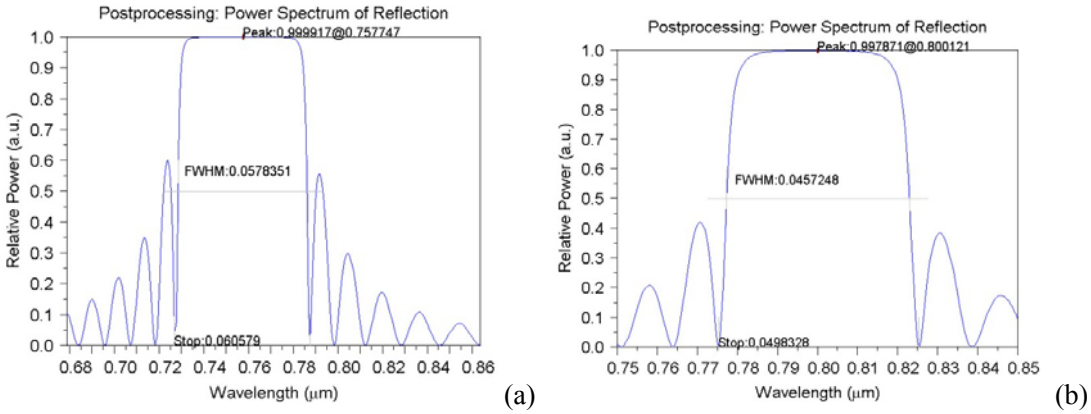

Figure 2.2 Power spectrum of reflection of (a) top etched grating and (b) lateral etched grating

The problem of this uniform laterally etching grating is that the side lobe reflection is quite severe. For example, the side lobe reflection of Figure 2.2 (b) is more than 40%. This will generate unnecessary reflection to the Raman scattering signals, which is detrimental to our measurement. In this program, we designed a new waveguide grating with apodization to minimize the side lobe reflection. Figure 2.3 (a) shows the design of a cosine type apodization grating, which has the same length (10μm) as the uniform grating in the previous report. The width of the grating is given by

$$width = 2 + (-1)^{floor(\frac{2z}{\Lambda})} \cos(\pi \left| \frac{z - \frac{L}{2}}{L} \right|) \qquad (2)$$

where Λ=0.5μm is the grating period, L=10μm is the total length. Figure 2.3 (b) shows the simulated reflection spectrum of the cosine type apodization grating with less than 1% side lobe reflection. The cost for this improvement is that the maximum reflection efficiency is reduced from 99.78% to 98.5%.

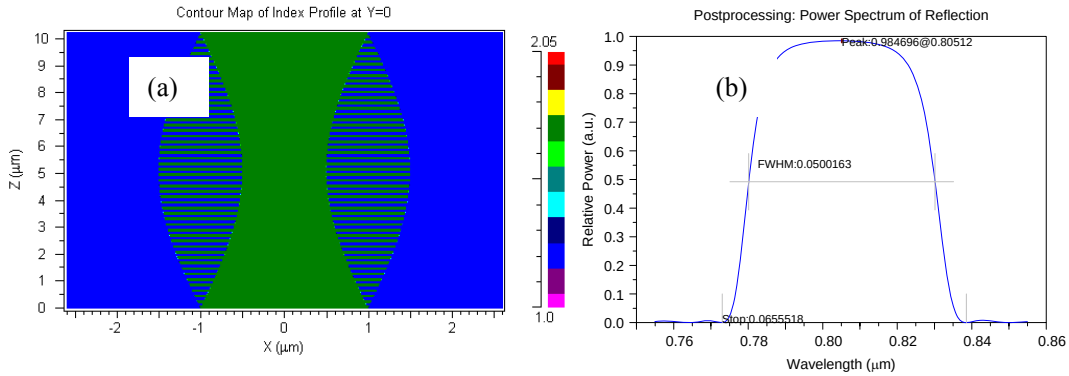

Figure 2.3 (a) Schematic design of the cosine type apodization grating (b) Reflection spectrum of the apodization grating with minimized side lobe

2.2 Fabrication of waveguide grating

The fabrication processes for the waveguide grating are given as the following steps, and schematically shown in Figure 2.4.

- We first deposit a layer of 3um thick SiO_2 on Si substrate
- We then deposit 0.6um thick Si_3N_4 on the SiO_2 layer
- We use E-beam lithography to write the inversed grating pattern on the e-beam photoresist that is spin coated on the Si_3N_4 and develop out the pattern
- We deposit 20nm Ni on the sample and put sample in PG remover for 2hs. This lift-off process will transfer the grating pattern with Ni as the hard mask
- We etch the Si_3N_4 using RIE with the Ni pattern as a mask

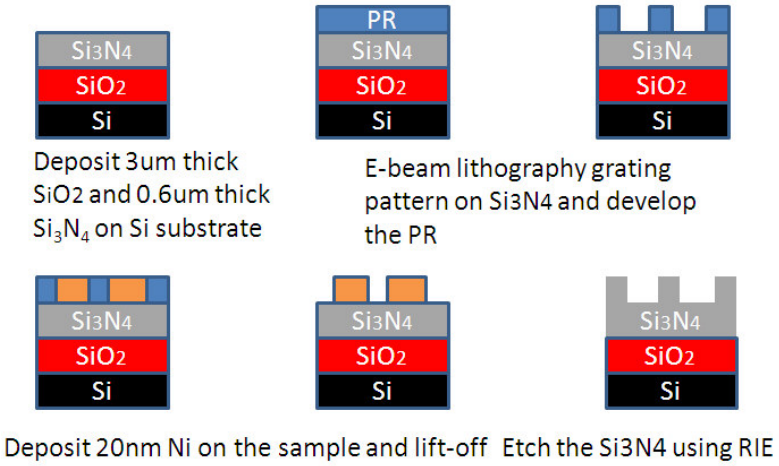

Figure 2.4 Fabrication processes for the waveguide grating on Si_3N_4

Figure 2.5 (a) and (b) shows the waveguide grating pattern after e-beam lithography and photoresist development, and the pattern after depositing Ni and the lift-off process.

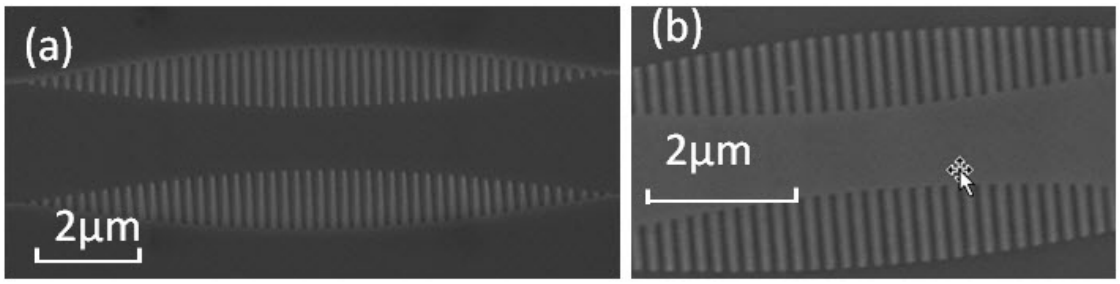

Figure 2.5 Waveguide grating patterns fabricated by e-beam photolithography and ion etching

2.3 Simulation of surface plasmonic resonance from gold nanowires

Electric field concentration between the gaps of nanowires provides the strongest Raman scattering enhancement for SERS measurement. In the Phase I program, we use two dimensional finite time domain difference (2-D FDTD) method to simulate the optical enhancement of nanowires with gaps. Then we use an analytical method to derivate 3-D

optical enhancement because 3-D FDTD simulation is very time consuming and has very high requirement on computer hardware.

In our 2-D FDTD simulation, we used a pair of 110nm long nanowires. To ensure sufficient supply of incident light energy, a large simulation window of 10μm*2μm is chosen and a wide light source of 10μm is used to illuminate the nanogap. The enhancement factor is given by comparing the optical intensity in the gap between and that in free space. Figure 2.6 shows the simulation results of the nanowires with 5nm gap. It is seen that the optical intensity is significantly enhanced.

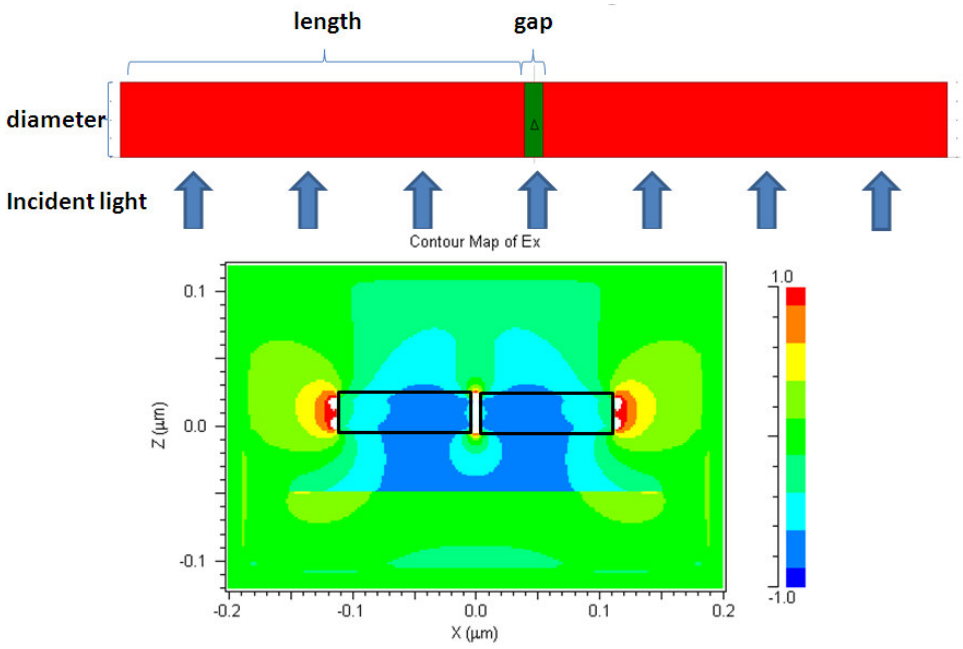

Figure 2.6 2-D FDTD simulation of optical enhancement of nanowires with gaps

Table 1 gives the enhancement factor of nanowires with different diameters and gap width. For large diameter (>30nm) nanowires, the strongest enhancement happens at 10nm gap; while for smaller diameter (10nm~25nm), the strongest enhancement happens at 5nm gap. This means there is a correlation between the nanowire diameter and the nano-gaps. It is seen that the maximum enhancement factor can be as high as 136. It might be possible that even higher enhancement can be achievable if the gap is smaller than 5nm. However, the fabrication process will become even more difficult. From the engineering point of view, 5nm gap is possibly the best choice when considering the combination of performance and fabrication ease. The enhancement factor in 2-D simulation means that the gaps can effectively absorb light in a space that is 136 times larger than that in the gap. If we consider 3-D cases, the gaps should be able to absorb light in a dimension that is $\pi/4\times136^2=14519$ times larger than the gap. Given the factor that SERS enhancement factor is quadratically proportional to the optical intensity; the estimated SERS enhancement factor for 3-D nanowires with 5nm gap should be at least 2×10^8. This matches reported experimental results very well.

Table 1 Simulation results of the optical intensity enhancement of nanowires with different diameters and gap width

$|E|^2$ Enhancement

diameter (nm) \ Gap(nm)	5	10	15	20	25
10	95.93	43.95	26.38	19.69	13.07
15	136.54	71.20	53.11	45.23	32.63
20	128.65	74.71	54.51	45.98	34.85
25	104.71	60.32	46.72	40.22	30.78
30	32.47	50.93	38.84	33.735	26.24

2.4 Fabrication of gold nanowires with nanogaps

Nanowires have been fabricated by electro-deposition through nanopores within a membrane made of alumina. The geometrical size and shape of the nanopores, whose diameters range from 20 to 400 nm with lengths up to the thickness of the membrane from a few to tens of micron, determine the dimensions of the nanowires. A Cu layer of 500 nm thick is first sputtered onto the back of the membrane to seal the pores and to serve as the working electrode in a three-electrode electro-deposition system as shown in Figure 2.7. An Ag/AgCl electrode works as reference electrode and A Pt mesh serves as counter electrode. An electric voltage is selected and applied between the working electrode and the reference electrode. Materials such as Ag, Au, and Ni can be readily electrodeposited into the nanopores and form into nanowires. Table.2 below lists the conditions that we used for the electro-deposition of Ag, Au, Cu, and Ni nanowires.

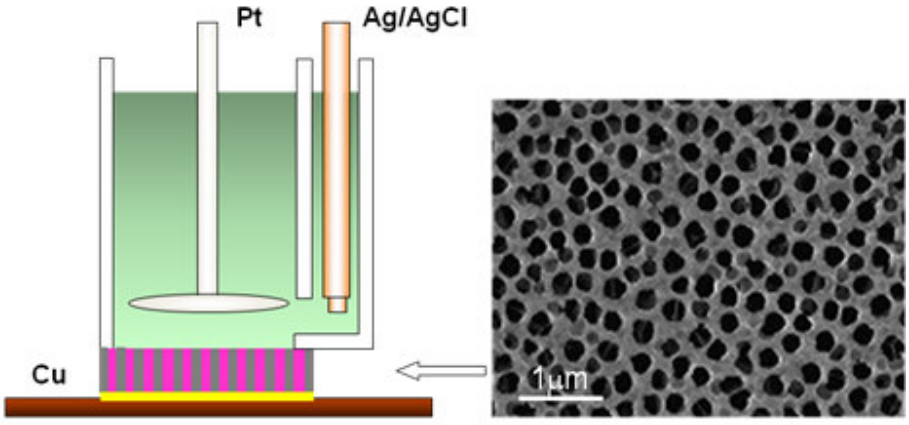

Figure 2.7 Three-electrode cell setup for electrodeposition of nanowires. A layer of Cu, sputtered at the back of the porous alumina templates serves as working electrode, Ag/AgCl serves as reference electrode, and Pt mesh serves as counter electrodes. Materials can be electrodeposited into the nanopores and form into nanowires

The electro-deposition of the nanowires commences at the bottom of the nanopores from the working electrode. The amount of electric charges passing through the circuit controls the length of the nanowires (or of the segments of a multi-segmented nanowire) in the membrane. Both single material (e.g., Au) and multi-segmented (e.g., AuNiAu-Ag-AuNiAu as shown in Figure 2.8) nanowires can be fabricated in this manner. After dissolving the membranes, using 2mol/l NaOH, the nanowires become free-standing and can be sonicated and centrifuged in ethanol and de-ionized (DI) water twice before re-suspended in DI water.

Table 2 Electro-deposition condition for the metallic nanowires

Materials	**Applied Voltage (V) (v.s. Ag/AgCl electrode)**	**Electrolyte composition**
Ag	-0.8	434 HS RTU, Technic Inc.
Au	-0.92	Techni Silver 1050, Technic Inc.
Cu	-0.15	A solution made of $CuSO_4.6H_2O$ and H_3BO_3
Ni	-0.9	A solution made of 20 g L^{-1} $NiCl_2.6H_2O$, 515 g $L^{-1}NiH_2NSO_3{\cdot}4H_2O$, 20 g L^{-1} H_3BO_3

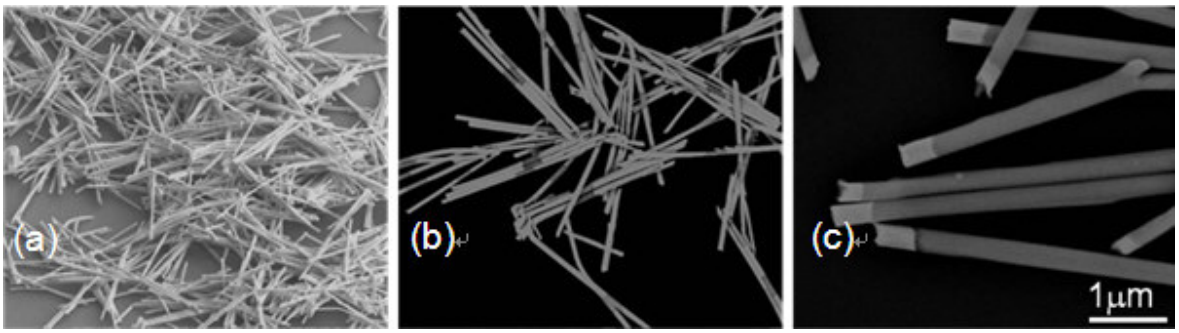

Figure 2.8 Both single material nanowires such as the Au nanowires in (a) and multisegmented nanowires such as the Au-Ni-Au nanowires in (b) and (c) can be electrodeposited.

2.5 Fabrication of nanogaps on nanowires

The nanogaps on nanowires were fabricated by on-wire-lithography. In brief, the nanogaps were created on multisegmented nanowires by sacrificial chemical etching of selected segments. Two approaches were examined for creating nanogaps. In the first approach, we used Cu segments as the sacrificial layers. In the second approach, we used Ag as the sacrificial layers. We successfully obtained nanogaps from 7nm to a few micrometers.

Approach 1: Fabrication of nanogaps by sacrificial etching of Cu segments

We started the fabrication with seven-segment nanowires made of Au/Ni/Au/Cu/Au/Ni/Au. The lengths of each Au and Ni segment were 0.75 μm. The length of Cu segment was 5 nm. Billions of nanowires have been synthesize with uniform diameters and lengths in each segment as shown in the backscattered SEM images in Figure 2.9 (a) and (b), where the Au segments are in bright and the Ni segments are in grey.

The Cu layer was identified by chemical etching with a solution made of 0.5 M copper chloride (CuCl2) and 0.1 M hydrochloride (HCl). We found that the Cu segment was etched away in the middle of two Au segments as shown in Figure 2.9 (c). However, we found two problems.

(1) We noticed that the Nickel segments were also partially etched as shown Figure 2.9(d).

(2) The smoothness of the interfaces between different materials is not satisfying due to the reaction of Cu layers with Au electrolyte during electro-deposition of the Au layers.

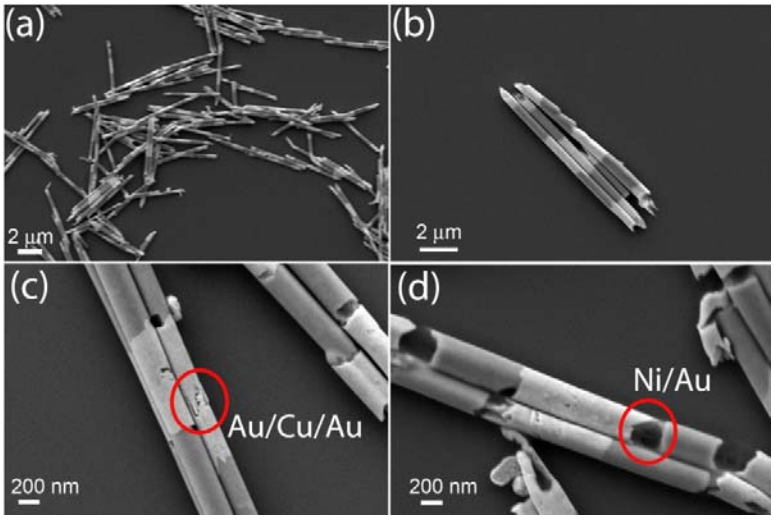

Figure 2.9 (a) Scanning Electron Microscope (SEM) images of as prepared Au/Ni/Au/Cu/Au/Ni/Au multi-segment nanowires. (b) The images obtained by back scattering show the Au segments in bright and the Ni segments in grey. (c) The Cu layer was identified by chemical etching with copper etchant made of 0.5 M copper chloride (CuCl2) and 0.1 M hydrochloride (HCl). (d)Part of the Ni layers was also etched.

We resolved these issues using the following two strategies:

(1) We used Ag segments in replace of the Cu segments. Ag is advantageous than Cu since it does not react with Au electrolyte and can be selectively etched with Ni and Au remain intact.

(2) We optimized the voltage and current density in the electrodeposition of Ag layers for smooth interfaces.

Approach 2: Fabrication of nanogaps by sacrificial etching of Ag segments

Multi-segment Au(0.75μm) /Ni (0.75μm)/Au(0.75μm)/Ag(7or30nm) /Au (0.75μm)Ni(0.75μm)/Au(0.75μm) nanowires were electrodeposited, where the Ag segments were used as the sacrificial layers for creation of the nano-gaps. Different from the Cu segments used in previous experiments, Ag remains intact in Au electrolyte during the deposition of the Au segments. As a result, the electrodeposited Ag segments have well controlled interface as shown in Figure 2.10 (a)-(b), which can be etched and form into narrow nanogaps. As shown in Figure 2.10 (c) and (d), we have obtained Ag

segments with 30±10 nm and 7±3 nm in length at 0.9 V (v.s. Ag/AgCl reference electrodes) by controlling the amount of charges passing through the circuit to be of -0.032 C and -0.016C, respectively.

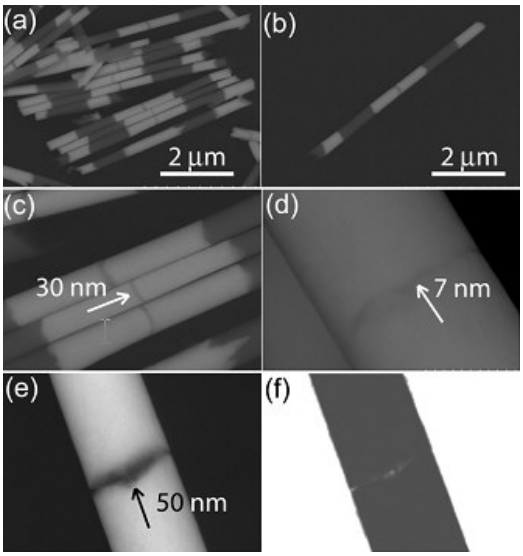

Figure 2.10 (a) and (b) SEM images of Multi-segment Au(0.75µm)/Ni(0.75µm)/Au(0.75µm)/Ag(7 or 30 nm) /Au(0.75µm)Ni(0.75µm) /Au(0.75µm) nanowires with Ag segments of (c)30±10 nm and (d) 7±3 nm . Selectively etching the Ag segments, nanogaps can be readily created with clean and smooth interfaces as shown in the (e) SEM and (f) TEM images.

The nanogaps were created on the nanowires by selective chemical etching of the Ag segments using a 4:1:1 mixture of methanol, H_2O_2 (30%), and NH_4OH. The structure of the nanogaps can be firmly fixed by a thin SiO_2 layer coated on the surface. Both the SEM [Figure 2.10(e)] and Tunneling Electron Microscopy (TEM) [Figure 2.10 (f)] images indicated the excellent quality of the narrow nanogaps with clear and smooth interfaces, which is most critical for achieving 10^8-time SERS enhancement.

2.6 Fabrication of nanogaps on nanowires with various diameters

The SERS enhancement factor not only depends on the sizes of the nanogaps but also on the diameters of the nanowires that the nanogaps are engraved on. Simulations show that smaller diameters of the nanowires should provide higher enhancement factors for SERS signal (Table 1). Therefore, it is highly desirable to obtain nanogaps on small-diameter nanowires. We successfully fabricated nanogaps on nanowires with 50-300 nm diameters by electro-deposition into templates with the same pore sizes. As shown in Figure 2.11 (a) and (b), arrays of multi-segmented nanowires of 50 nm in diameters have been synthesized and uniformly dispersed on silicon substrate. In comparison, most of the nanogap structures that are published previously were only obtained on nanowires of 200-300 nm in diameters.

In summary, we have demonstrated the synthesis of nanogaps of 7 nm to 30 nm on nanowires of 50 nm to 300 nm in diameter. Both the sizes of the nanogaps and the diameters of the nanowires can be tuned for optimal enhancement of Surface Enhanced Raman Scattering (SERS). This result represents a great technical improvement in the controlling of the dimensions of the nanowire-nanogap structures for SERS measurement.

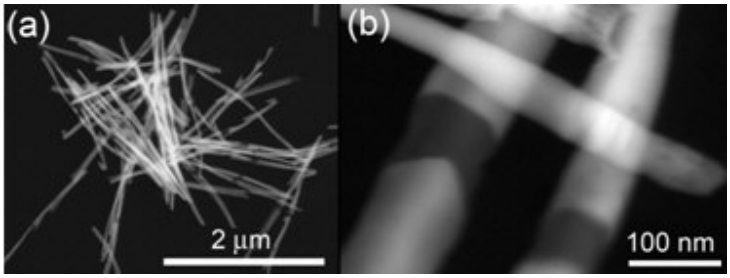

Figure 2.11 Nanogap-on-nanowire structures using on-wire-lithography with the nanogaps range from 7 nm to 50 nm and the nanowires with diameters from 50 nm to 300 nm. As shown in (a) and (b), the nanogaps have been made on the 50 nm-diameter nanowires

2.7 Measurement of SERS from nanogaps

We used a custom-built Raman Microscope shown in Figure 2.12 for detection of the SERS signals from the nanogap-on-nanowire structures. The Raman Microscope consists of an Olympus IX-71 Inverted Microscope with lasers of wavelengths of 512 to 633 nm as the excitation source. The signal was collected and analyzed by a 50cm Spectrometer equipped with a liquid-nitrogen cooled CCD camera (1340x 400) made by Princeton Instrument Inc. The edge filters were set in the 6-position turret in the optical path which can selectively pass the Raman signals and reject the excitation lasers.

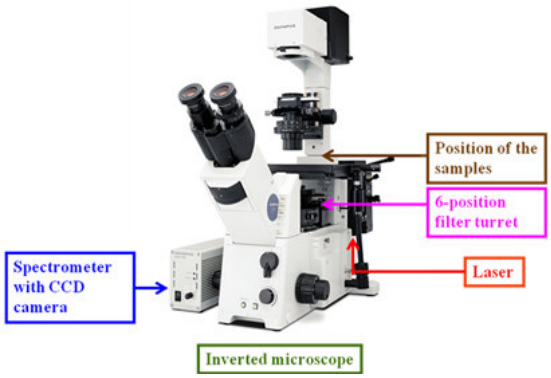

Figure 2.12 Custom built Raman microscope for the detection of SERS signals from the metallic nano-structure

In order to select the best excitation wavelength for the enhanced SERS signals, we first test the plasmonic resonance frequency of the nanogap structures using dark field imaging technique. A full-spectrum white light was directed on the nanogaps, from which the reflected light was collected and analyzed by a spectrometer equipped with a CCD

camera. As shown in Figure 2.13(a), arrays of nanogaps are shown in the dark-field image. Resolving one of them, the maximum extinction frequency can be determined to be at 725 nm for 50-nm nanogaps on 100-nm nanowires [Figure 2.13(b)]. At this specific frequency, the electrons in the nanogap-nanowire structures resonate with external optical light, resulting in the maximum absorption of laser by the nanogaps. It enhances the SERS signals to the highest extent. According to this result, we selected a laser source with wavelength of 633 nm for SERS excitation. This is the best laser that matches the resonance frequency. We successfully detected SERS signals of 1mM MeMethylene Blue functionalized on a few aggregated nanogaps as shown in Figure 2.13(c). The spectra, in agreement with that of the standard data for Methylene Blue, proved that our nanogap structures can significantly enhanced the SERS signals by 10^8 times. Additionally, we have obtained SERS signals from various nanogap-on-nanowire structures as shown in Figure 2.13(c). The maximum enhancement occurred on the samples with 10-nm nanogaps on 50 nm diameter nanowires. As a result, our work readily demonstrates the feasibility of SERS detection of biochemical entities based on nanogap structures.

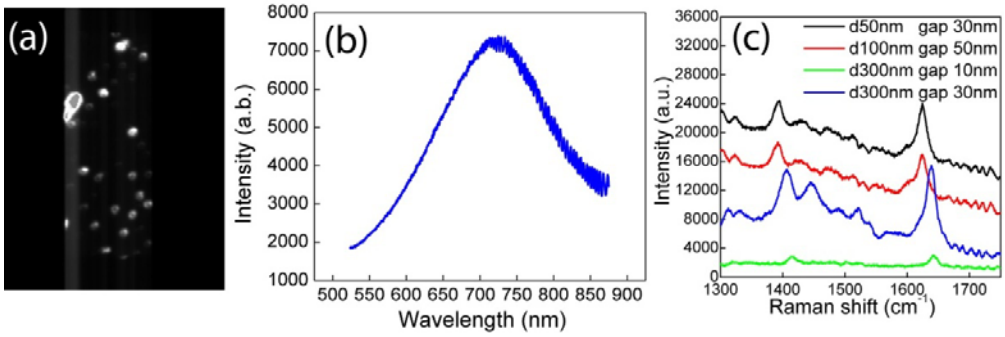

Figure 2.13 (a) Dark field image of the 50nm-nanogaps on 100 nm nanowires. (b) Plasmonic Resonance Frequency was determined to be 725 nm for the same type of nanogaps. (c) The SERS signals of Methylene Blue have been successfully detected from various sized nanogap- nanowire structures.

3. *Phase II Plan*

As the feasibility of the proposed on-chip SERS spectrometer has been proved in Phase I, the Phase II program will focus on the full implementation of the proposed on-chip SERS spectrometer in a step-by-step manner, and eventually fulfill a high level integration of the on-chip spectrometer with minimized size and weight. The application of such a highly integrated SERS spectrometer array for single molecule detection of multiple analytes will also be investigated. Specifically, the work in Phase II program will target at the following objectives:

- Testing and characterization of high reflectivity Si_3N_4 waveguide gratings and high-Q resonant cavity with ultra compact size
- Simulation and investigation of the optical intensity enhancement from gold nanowires with different diameters and gap widths. An optimized design with

acceptable engineering feasibility should be given by a highly accurate 3-D FDTD simulation method

- Building-up of a reconfigurable Raman microscope for both free space and guided wave Raman scattering measurement
- Fabrication and characterization of the proposed on-chip SERS spectrometer array usingguided wave photonic devices and metallic nanowires with nano-gaps. Electric tweezers will function as the bridge to link these two different technical subjects. For this most pivotal technical objective, we will divide it into several sub-objectives with increasing complexity with ensure a feasible and stable pace for research and development progress. These sub-objectives are listed as:
  1) Surface Enhanced Raman Scattering (SERS) measurement based on gold nanowires and Si_3N_4 waveguides
  2) SERS measurement based on gold nanowires and high-Q resonant cavity
  3) SERS spectrometer array based on gold nanowires and high-Q resonant cavity array
- Single molecule detection for multiple analytes through Functionalization of different gold nanowires
- High level integration of on-chip SERS spectrometer and characterization
- Design and implement an advanced fiber-optic coupling method through tapered waveguide structure, estimating a total loss reduction around 8dB
- Packaging and reliability evaluation

These objectives shall lay a solid foundation for the full implementation of an on-chip SERS spectrometer (array) and commercialization using the proposed technological approaches and, potentially, the widespread presence of guide wave photonic device based SERS spectrometer with reduced cost and enhanced performance. The corresponding tasks to realize these objectives are further delineated in the Phase II proposal.